Effect of water saturation on the diffusion/adsorption of ^{22}Na and cesium onto the Callovo-Oxfordian Claystones

S. Savoye[*, a], S. Lefevre[a], A. Fayette[a], and J.C. Robinet[b]

[a] *DEN-Service d'Etude du Comportement des Radionucléides (SECR), CEA, Université Paris-Saclay, F-91191 Gif-sur-Yvette, France*

[b] *R&D Division, Transfert Unit, Andra, F-92298 Châtenay-Malabry, France*

* Corresponding author: *sebastien.savoye@cea.fr*

Key words: sodium, cesium, diffusion, unsaturated clay materials, adsorption, Callovo-Oxfordian shales

ABSTRACT

The diffusion and adsorption behaviors of sodium and cesium were investigated in the Callovo-Oxfordian claystone (France) under unsaturated conditions. Through-, out- and in-diffusion laboratory experiments were performed on intact and compacted samples partially-saturated by means of the osmotic method for imposed suction up to 9 MPa. These specific devices led to values of water saturation degree ranging from 81% to 100% for intact samples and from 70% to 100% for compacted materials. The results showed a very low impact of water saturation on the extent of adsorption for ^{22}Na and cesium, onto both intact and compacted materials, suggesting that the saturation degrees were not enough low to limit the access of cations to adsorption sites on clay surfaces. At full saturation, enhanced diffusion for ^{22}Na and cesium was clearly evidenced on intact samples with diffusivity 4 and 10 times higher than that of tritiated water (HTO), respectively, in accordance with previous works. The same tendency was also observed on compacted materials, with a diffusivity 4 times higher for cesium than for sodium. Under unsaturated conditions, the diffusion was slower than that in fully-saturated samples. The diffuse behavior under unsaturated conditions is clearly distinct between cesium and sodium. For the intact rock and under 1.9 MPa of suction, the diffusivity of cesium is reduced by a factor 17, whereas for sodium, it is reduced by a factor of 5. In the compacted materials (under 1.9 MPa of suction), this difference is enhanced with a decrease of the diffusivity by a factor 47 and 6 for cesium and sodium, respectively. Finally, a literature review has been performed to explain the differences of diffusive behavior between cesium and sodium under unsaturated conditions.

INTRODUCTION

Geological clayey formations are widely being investigated by several countries in the world for hosting radioactive waste disposal facilities (Andra, 2005; Hendry *et al.* 2015). Indeed, their very low permeability limits the radionuclide transfer to the very slow diffusive process, and clay minerals present within these rocks are capable of strongly adsorbing cationic radionuclides. Therefore, both properties drastically could slow down radionuclide migration towards the biosphere.

However, there are many cases where the soils or the rocks surrounding such waste disposal facilities can be unsaturated, leading to potential change of their containment properties. For example, many landfills are constructed in arid or semi-arid environments, where the soil can be unsaturated at great depths (Fityus *et al.* 1999). In the case of deep argillaceous formations such as the Callovo-Oxfordian claystones studied by the French Waste Management Agency (Andra), the presence of a radioactive waste repository is expected to induce a hydraulic disequilibrium in the near-field of the host-rocks. Initially, ventilation of the underground drifts and shafts during the construction and the operation phase would lead to the partial dehydration of the rock around the drift (Andra 2005; Armand *et al.* 2014). Then, after a re-saturation phase, the anoxic corrosion of the canisters would produce hydrogen inducing unsaturated conditions in the near field of the claystones again (Marschall *et al.* 2005). Hence, it is important to understand how unsaturated conditions can impact radionuclide migration through these formations, *i.e.*, in terms of diffusion and adsorption processes.

However, since performing diffusion/retention experiments through water-saturated rocks is already a challenging task, especially through these low permeability clay rocks (*e.g.*, Van Loon *et al.* 2004; Hendry *et al.* 2015; Savoye *et al.* 2015), a few diffusion/retention experiments carried out under partially saturated conditions are reported in literature. Most of the diffusion testing is based on the half-cell method (Schaefer et al. 1995; Hamamoto *et al.* 2009; Aldaba *et al.* 2010; Tokunaga *et al.* 2017), known to generate artifacts due to the partial contact between the two half-cells (Shackelford 1991). Recently, we presented an innovative technique allowing the diffusion of uncharged tritiated water (HTO) and solutes through unsaturated Callovo-Oxfordian (COx) argillaceous rocks (Savoye *et al.* 2010, 2012a) and compacted materials with variable clay content (Savoye *et al.* 2014). In these previous studies, the water saturation degree is imposed by osmosis process. Through-diffusion method was then used for investigating the diffusive behavior of HTO and anionic species ($^{125}I^-$), while the decreasing source concentration method or transient in-diffusion method was applied for characterizing the diffusion/adsorption of cesium (See Shackelford 1991 for details about these techniques).

All these studies revealed a very sharp decrease of the effective diffusion coefficients (D_e), especially for cesium. For instance, when dehydrating intact COx samples down to 81% of saturation, D_e values were reduced by a factor of 7 for HTO, by a factor of 50 for iodide, and by a factor of about 60 for cesium. The cesium decrease was almost 1 order of magnitude higher than that for tritiated water (HTO). This behavior was still unexplained, since cesium and HTO were expected to diffuse in the same volume of the pore space, in fully saturated claystones. Therefore, several hypotheses have been proposed to explain such an unexpected difference. First, diffusion of HTO under partially-saturated conditions could occur in liquid phase but also in vapor phase, contrary to solutes such as cesium that would have been forced to diffuse in liquid phase only. Therefore such a property would reduce its diffusive pathway within sample, and would reduce the extent of its diffusivity drop with

respect to cesium. On the other hand, the larger cesium diffusivity drop could be related to the inhibition of the so-called surface diffusion when dehydrating. Surface diffusion has been used to explain the too high cation flux in fully-saturated conditions, compared to what can be predicted from a simple pore diffusion model using water diffusion coefficient (Melkior *et al.* 2005, 2007; Gimmi & Kosakowski 2011). Therefore, this reduction would then necessarily have to be related to a decrease of clay surface accessibility due to dehydration, leading to a reduction of the amount of adsorbed cesium, responsible for the enhanced diffusion at full saturation.

In order to address this issue, the present study aims at properly determining the extent of the diffusive/adsorption behavior of two cations (*i.e.*, ^{22}Na and cesium) onto partially saturated clayrocks under intact or compacted state. ^{22}Na was chosen because it is a weakly-adsorbed cation, known to be less impacted by surface diffusion mechanisms than cesium at full-saturation (Melkior *et al.* 2005, 2007; Gimmi & Kosakowski 2011). Its diffusive behavior is thus expected to be "intermediate" between cesium and HTO. The study of two sample states (intact and compacted) aims at (i) verifying whether the consistency of the adsorption extent observed at full saturation on intact and compacted samples is still valid under partial water saturated conditions (see Chen *et al.* 2014 for adsorption of cesium onto full-saturated Callovo-Oxfordian claystones) and (ii) investigating the role played by the pore network geometry on diffusion under partially-saturated conditions.

Therefore, several diffusive techniques were used for acquiring both diffusion coefficients and the extent of cation adsorption under experimental conditions identical to those previously used in Savoye *et al.* (2010, 2012a): (i) rock samples issued from core in the immediate vicinity with the one used in the previous studies and (ii) use of the same four suctions (up to 9 MPa) previously generated by osmosis process. Acquisition of proper cation adsorption values was achieved using the principle of the diffusive method developed by Montavon *et al.* (2006) and adapted to partially saturated conditions. In this case, the decreasing source concentration method was allowed to fully reach cation concentration equilibrium between reservoir and rock sample, and at the end of the experiment, cation concentration was measured within rock sample by means of abrasive peeling technique developed by Van Loon & Eikenberg (2005). In addition to the "in-diffusion until equilibrium" method, through- and out-diffusion techniques were also used for investigating the diffusion of ^{22}Na through intact rock samples. All these experiments enabled us to obtain a direct comparison of the diffusive/adsorption behavior of two types of cations (sodium and cesium) as a function of the saturation degree.

MATERIALS AND METHODS

Sample origin and sample preparation.

The rock samples used for the measurements originated from the Callovo-Oxfordian sedimentary formation (COx) located in eastern part of the Paris basin. The Callovo-Oxfordian formation has been selected by France to host a deep underground nuclear waste repository and is currently studied by Andra in Meuse/Haute Marne Underground Research Laboratory (URL). The mineralogy of the COx is mainly constituted by clay minerals (illite, illite/smectite mixed-layered mineral, chlorite and kaolinite), quartz and carbonates (Gaucher *et al.* 2004). The core sample referenced EST27340 (484.5 - 484.8 m bgl) was selected for this study. It originates from a borehole cored from the main shaft of the Meuse/Haute Marne URL (490 m bgl). The EST27340 core sample is located at the immediate vicinity of the core studied by Savoye *et al.* (2010, 2012a) for determining the diffusive behavior of

HTO, ^{125}I and Cs through intact partially-saturated clayrock samples. The mineral and microstructural properties of these two cores are expected to be very similar, leading to comparable diffusion/adsorption properties.

For the study of intact materials, eight samples were sliced from the EST27340 core using a diamond wire saw (no lubricating fluid was used) into pieces so that the diffusion would occur perpendicular to the bedding planes. Four samples dedicated to ^{22}Na through- and out-diffusion experiments were then placed on a lathe to obtain 36-mm diameter disks and four ones dedicated to "in-diffusion until equilibrium" experiments and petrophysical measurement to obtain 18.75 mm-diameter disks. For the study of compacted materials, pieces of EST27340 core were crushed and sieved (100 µm mesh). All the sliced samples and the powder were stored at 30.0 ± 0.2 °C in desiccators containing a NaCl-oversaturated solution (suction = 39 MPa), until suction equilibrium, which was achieved after *ca.* 3 months (indicated by mass stabilization). Callovo-Oxfordian powder was then directly compacted into the in-diffusion cells at a dry density of 1.6 g cm^{-3}, while the dry density of intact COx sample was equal to 2.19±0.20 g cm^{-3} as determined by Savoye *et al.* (2010). Note that for the "in-diffusion until equilibrium" experiments, the sample thickness was adapted from 10 mm to 2 mm to minimize the achievement of the equilibrium state, while the samples dedicated to through- and out-diffusion and petrophysical measurements were about 1cm-thick (see Table 1).

Desaturation procedure

The suction is generated by the osmosis process between the pore-water (present in the pores of the sample) and a highly concentrated solution with large-sized molecules of polyethylene glycol (PEG; for more details see Savoye *et al.* 2010). The sample is separated from the PEG-solution by a semipermeable membrane (which is permeable to all except PEG). The exclusion of the PEG from the sample results in a chemical-potential imbalance between the water in the clay sample and the water in the reservoir chambers. This osmotic suction has the effect of keeping the sample unsaturated. Moreover, the value of the imposed suction and thus the saturation state of the sample depend on the PEG concentration in solution (Delage *et al.* 1998). The different saturation states were reached with chemical solutions prepared with Increasing PEG concentrations (0, 0.42, 0.76, and 0.95 g per g of solution), leading to increasing suction values (0, 1.9, 6.3 and 9 MPa, respectively) (Savoye *et al.* 2010, 2012a, 2014). Semi-permeable membranes with 3500 g mol^{-1} molecular weight cut-off (MWCO) were chosen in order to prevent the PEG 6000 (*i.e.*, 6000 g mol^{-1} molecular weight) from bypassing the membranes.

The 36-mm-diameter samples used for through-and out-diffusion experiments were inserted in a stainless steel holder, and were sandwiched between two semi-permeable membranes fabricated of cellulose acetate (Spectra-Por 3500 Da, Spectrum laboratories, USA). Afterwards, two polyetheretherketone (PEEK) grids (Polyetheretherketone – Mesh, Goodfellow, England) with 60 and 45 meshes were put between the o-rings to limit the dead-volume. Then, the two end-pieces were placed in position. See Savoye *et al.* (2010, 2012a) for details about the set-up. For the "in-diffusion until equilibrium" set-up, intact and compacted samples were placed in PEEK holders, sandwiched between two semi-permeable membranes and two stainless-steel filters. See Altmann *et al.* (2015) for a detail description of this set-up.

For osmotic re-saturation, solutions were prepared with ultrapure deionised water (18.2 MΩ cm^{-1}), PEG 6000 (Merck, Germany), and commercial salts (American Chemical Society reagent grade or

higher quality and purity salts), so as to obtain a chemical composition as close as possible to the pore-water one. The recipe was based on the chemical composition measured from in situ water sampling performed at a level close to the sampling level of this study (475m bgl) (Vinsot *et al.* 2008). The total concentrations for calcium, magnesium, potassium and sodium were 3.0, 2.0, 1.7, and 51.6 mmol L^{-1}, respectively. The anion concentrations for chloride, sulfate and the carbonate species were 41.0, 11.0 and 0.70 mmol L^{-1}, respectively.

For the through- and out-diffusion experiment, the experimental set-up comprises a diffusion cell, a 16-channel peristaltic pump (IPS, Ismatec, Idex Corporation, USA), and a 200-cm3 reservoir. During the hydric equilibrium phase, both sides of the samples were in contact with the same synthetic water and PEG solution, using a unique reservoir. For the "in-diffusion until equilibrium" experiment, the set-up is limited to the PEEK diffusion cell which was directly emplaced in a source reservoir for the hydric equilibrium step. One month was shown to be sufficient to achieve the hydric equilibrium for the rock sample (Savoye *et al.* 2010), before starting either the dismantling of the cells for performing the petrophysical measurements or the diffusion tests (described below).

Petrophysical measurements

In order to determine the water content and the degree of saturation as a function of imposed suctions, petrophysical measurements have been performed as follows: (i) water contents (w) were measured by weighing before and after oven-heating at 105°C for 48 h and were described on a mass basis relative to the wet mass; (ii) bulk dry density ρ_d was determined by measuring the pressure exerted by the sample immersed in kerosene according to Archimedes' principle (Savoye *et al.* 2008); and (iii) grain density was determined in a Micrometrics Accupyc 1330 helium pycnometer.

The volumetric moisture content, θ, is calculated from the water content by using the following expression (Savoye *et al.* 2006):

$$\theta = \frac{w \times \rho_s}{(1-w) \times \rho_w + w \times \rho_s} \quad (1)$$

Where ρ_w = the density of the pore water (1 g cm^{-3}) and ρ_s = the measured grain density of the rock ((2.7023 ± 0.0016) g cm^{-3}, Savoye *et al.* 2010).

The total porosity is deduced from the following equation:

$$\phi = 1 - \frac{\rho_{bulk,dry}}{\rho_s} \quad (2)$$

Finally, the saturation degree (S_w) corresponds to the ratio of volumetric water content (θ) over the total porosity (ϕ).

Protocols for the diffusion experiments

After one month of saturation treatment, cells devoted to through- and out-diffusion experiments were connected to two distinct reservoirs. The upstream reservoir was filled with 100 cm^3 of a fresh solution labelled with ^{22}Na, and a 20-cm^3-downstream reservoir filled with a fresh solution without tracer was connected to the cell. During the through-diffusion step, the solution in the downstream

reservoir was regularly replaced in order to maintain the lowest tracer concentration as reasonably possible, *i.e.*, less than 3% of the one measured in the upstream reservoir. On the other hand, the concentration in the upstream reservoir was left free to decrease. After completion of the through-diffusion stage, an out-diffusion procedure was applied to study the reversibility behavior of ^{22}Na diffusing out of the rock sample. The solutions in both reservoirs were fully replaced by synthetic solutions without tracer to make ^{22}Na diffuse out of the rock samples. At selected time intervals, the activity in the solutions was measured for monitoring the activity rate at which the tracers came out of the samples (see Savoye *et al.* 2015 for details).

For the cells devoted to the "in-diffusion until equilibrium" experiments, their source reservoir was filled with fresh solution labelled either with ^{22}Na or ^{134}Cs + 8.10^{-4} mol L^{-1} of pure water of CsCl. This value of 8.10^{-4} mol L^{-1} of pure water was chosen so that the equilibrated cesium concentration should be close to 5.10^{-4} mol L^{-1} of pure water, by assuming a K_D value of 26 L kg^{-1} (see Eq (3) below) estimating from Savoye *et al.* (2012a). Due to the higher affinity of cesium towards rock sample than sodium, a larger solution volume of 0.11 L of pure water was chosen than for sodium (0.03 L of pure water). At selected time intervals, the activity in the solutions was measured for determining the achievement of the equilibration step. Afterwards, the diffusion cells were dismantled and the rock samples were dried at 105° C for 24 h. Then, the ^{22}Na and ^{134}Cs profiles in the rock were acquired using the high-resolution abrasive peeling method developed by Van Loon & Eikenberg (2005). The principle of this technique is the removal of thin layers of the rock sample by abrading the material on grinding paper. This powder is then recovered by water leaching and transferred into a tube directly used for γ counting. The sample thickness was measured using a micrometer (Mitutoyo, Japan) after each grinding.

The activities for ^{22}Na and ^{134}Cs were counted by γ counter (Packard 1480 WIZARD, USA). ^{22}Na and ^{134}Cs data were corrected for radioactive decay with respect to the tracer injection time. A summary of the samples, the types of the experiment, and the studied species was reported in Table 1.

Treatment of experimental results

For the "in-diffusion until equilibrium" experiments, two types of treatment were used for the interpretation of the data. Indeed, since the equilibrium is assumed to be reached between solution and solid phase, the distribution coefficient, K_D (L kg^{-1}) can be directly calculated from the estimation of the rock concentration from abrasive peeling and the final concentration measured in solution, by the following relationship:

$$K_D = \frac{C_{solid}}{C_{eq\_solution}} \quad (3)$$

Where C_{solid} is the concentration of tracer adsorbed on solid (mol kg^{-1} of dry sample) and $C_{eq\_solution}$ is the final concentration of tracer remaining in solution (mol L^{-1} of pure water).

In addition to this direct approach, the application of the Fick's second law for one-dimensional transport can be used:

$$\frac{\partial C}{\partial t} = \frac{D_e}{\alpha}\frac{\partial^2 C}{\partial x^2} = \frac{D_e}{\varepsilon_a + \rho_d K_D}\frac{\partial^2 C}{\partial x^2} \quad (4)$$

Where C is the concentration or activity per mass unit in the solute phase (mol m^{-3} of pure water or Bq m^{-3} of pure water); t, the time (s); D_e, the effective diffusion coefficient (m^2 s^{-1}); ε_a, the diffusion-accessible porosity (m^3 m^{-3}); ρ_d, the bulk dry density (kg m^{-3}).

The K_D value was calculated from the relationship $K_D = (\alpha - \varepsilon_a)/\rho_d$, by assuming that the accessible porosities of ^{22}Na and cesium were identical to the volumetric moisure content, *i.e.,* $\varepsilon_a = \theta = \phi \cdot S_w$.

Therefore, depending on the type of diffusion experiments, different boundary and initial conditions have to be considered.

For the through-diffusion system used for ^{22}Na, boundary and initial conditions are as follows:

$$C(x, t) = 0, \qquad t = 0 \tag{5}$$

$$C(x, t) = C_0, \qquad x = 0,\ t = 0 \tag{6}$$

$$C(x, t) = 0, \qquad x = L,\ t > 0 \tag{7}$$

Where L is the sample thickness (m) and C_0 is the concentration of the tracer in the upstream reservoir (mol m^{-3} of pure water or Bq m^{-3} of pure water). Fully analytical solutions for through-diffusion and reservoir-depletion studies are obtained in the Laplace space, which are subsequently numerically inverted to provide the solution in time (Moridis, 1998).

For the out-diffusion stage, Eq. (4) has to be solved with the corresponding boundary conditions:

$$C(0,t) = C(L,t) = 0, \quad t>0 \tag{8}$$

For the analytical approach, we can assume that the concentration gradient across the sample is linear when the through-diffusion stage reaches the steady-state, the concentration profile that gives the initial conditions for out-diffusion, is:

$$C(x) = C_{TD\_end}\ (1 - \frac{x}{L}) \tag{9}$$

Where C_{TD_end} is the concentration of tracer in the upstream reservoir at the end of the through-diffusion step (mol m^{-3} of pure water or Bq m^{-3} of pure water).

According to Jakob *et al.* (1999), the total amount of tracer (mol or Bq) diffused out of the sample at the two boundaries is given by:

at $x = 0$: $$A(0,t) = 2 \cdot C_{TD\_end} \cdot S \cdot \alpha \cdot L \left[\frac{1}{6} - \sum_{n=1}^{\infty} \frac{1}{\pi^2 n^2} e^{-\left(\frac{n\cdot\pi}{L}\right)^2 \cdot \frac{D_e}{\alpha} \cdot t} \right] \tag{10}$$

and

at $x = L$: $$A(L,t) = 2 \cdot C_{TD\_end} \cdot S \cdot \alpha \cdot L \left[\frac{1}{12} + \sum_{n=1}^{\infty} \frac{(-1)^n}{\pi^2 n^2} \cdot e^{-\left(\frac{n\cdot\pi}{L}\right)^2 \cdot \frac{D_e}{\alpha} \cdot t} \right] \tag{11}$$

Where *S* is the surface of the rock sample (m^2).

Lastly, for the "in-diffusion until equilibrium" case, the boundary and initial conditions are as follows:

$$C(x, t) = 0, \qquad t = 0 \tag{12}$$

$$C(x, t) = C_0, \qquad x = 0,\ t = 0 \tag{13}$$

$$\frac{\partial C}{\partial x} = 0, \qquad x = L,\ t \geq 0 \tag{14}$$

Note that in this case, both for intact and compacted materials, the presence of steel filterplate was taken into account in the semi-analytical solution, using the following input parameters: thickness: 1.95 mm; filterplate geometry factor, D_0/D_e = 8.19 given by Descostes *et al.* (2008); porosity: 37%; D_0, self-diffusion coefficients for Na and Cs from Savoye *et al.* (2011).

Uncertainties on the experimental data were estimated by propagation of the analytical error variances (σ^2_{V1}, σ^2_{V2}, etc…) following the Gaussian error propagation law. The approaches used for determining the uncertainties on the experimental data and the error range of the diffusive parameters are described in Savoye *et al.* (2012b)

RESULTS

Petrophysical data

Figure 1 shows the evolution as a function of the imposed suction of the saturation degrees measured on compacted materials and on intact rock samples. The application of suction up to 9MPa allowed the intact samples to be dehydrated down to 81% and the compacted samples down to 70%. Note a good consistency of the saturation degrees determined on intact rock samples at the highest suction by Savoye *et al.* (2010) and in the present study. Moreover, for each suction level strictly higher than 0 MPa, compacted materials display saturation degree values about 10% lower than the ones measured on the intact materials. In comparison to the intact rock, the pore size distribution in compacted materials at ρ_d equal to 1.6 g cm^{-3} is characterized by larger pore diameters (see *e.g.*, Fig. 9 in Tang *et al.*, 2011). Consequently, in agreement with the Jurin-Laplace's law, a lower saturation degree is expected in compacted materials for a same suction. One issue to address is to know whether dehydration is able to limit the accessibility of cations present in pore-water to clay surfaces (including interlayer space).

^{22}Na diffusion experiments

Figure 2 (A-B) shows the normalized activity in downstream reservoir and the normalized instant flux in upstream reservoir for the four through-diffusion experiments performed with ^{22}Na on intact clay rocks (S_w = 81, 86, 89 & 100 %). The effect of desaturation is (i) to slow down the activity decrease in the downstream and (ii) to decrease the instant flux relative from the full-saturated sample to the more de-saturated one. For example, incoming flux decreases by a factor of approximately 20 for ^{22}Na from full-saturation to 81 % of saturation.

Interpretation of such dataset is classically achieved by means of a least square fitting of the model to both the incoming flux in the downstream reservoir and activity decrease in the upstream

reservoir. However, this approach was only applicable to through-diffusion experiment carried out into fully-saturated sample (Figure 2) with the associated diffusive parameters given in Table 2. Therefore, we performed a separate fitting approach to interpret either the activity decrease or the incoming flux. Note that the fitting approach based on the activity decrease led to diffusive parameters with larger uncertainty range than the one based on the incoming flux. Indeed, the former approach only enables an estimation of the apparent diffusion coefficient (D_a) defined as D_e/α. In order to constrain α values, and thus corresponding K_D values from interpretation of activity decrease, two extreme conditions were considered for D_e values: (i) using the same D_e values as the ones calculated from the downstream modelling (dotted line) and (ii) using D_e values preventing the simulated incoming flux from being higher than the experimental one (dashed line). The corresponding K_D values calculated from the relationship $K_D = (\alpha - \theta)/\rho_d$, were also reported in Table 2.

In Figure 2, for partially-saturated samples, the higher the desaturation, the larger the discrepancy between simulated curves (solid lines) calculated from incoming flux show and the experimental data acquired in the upstream reservoir. In this case, simulated curves underestimated the activity decrease in upstream reservoir (Figure 2 (A)), suggesting that more ^{22}Na would diffuse into partially-saturated samples than ^{22}Na that would diffuse out. Note that no such discrepancy between upstream and downstream reservoirs had been observed when tritiated water or $^{125}I^-$ diffused through partially saturated COx samples (Savoye *et al.* 2010). Moreover, simulations carried out from an interpretation of activity decrease were able to well reproduce data in upstream reservoir, but failed to reproduce the incoming flux in downstream reservoir (Figure 2). This clearly confirms the distinct behavior of ^{22}Na diffusing into the dehydrated samples and the one diffusing out.

Regarding out-diffusion experiment results, the evolution of total diffused activity measured in upstream and downstream reservoirs was reported in Figure 3. It is noteworthy that, for the two experiments carried out at 86% and 89% of saturation, after almost 300 days, there was still some fresh ^{22}Na diffusing out the samples, since no plateau was yet reached. The associated simulated curves were calculated using Eqs (10) and (11) with the diffusive parameter values given in Table 2. The D_e values estimated from out-diffusion experiments are relatively well consistent with those estimated from the analysis of the incoming flux for through-diffusion experiments (Table 2).

The results obtained from the "in-diffusion until equilibrium" experiment carried out on intact clayrock sample at 81% of saturation are reported in Figure 4 (A-B). Figure 4 (A) shows the evolution of ^{22}Na specific activity in the source reservoir as a function of time with the associated modeled curves, while ^{22}Na rock profile activity was given in Figure 4 (B). By means of the ^{22}Na rock profile activity and the last measured specific activity in solution, it is possible to use Eq (3) to directly estimate the K_D value, given in Table 3. Note that in Eq (3), C_{solid} corresponds to the concentration of adsorbed ^{22}Na on solid, excluding the ^{22}Na activity remaining in porewater. Using this 'rock' K_D value, the activity evolution in solution can be modelled with D_e value given in Table 3. One can notice that (i) the activity decrease in solution is very well reproduced with such 'rock' K_D and (ii) the D_e value (2.5×10^{-12} m² s^{-1}) is very close to the ones estimated from through- and out-diffusion experiment (3-1.5×10^{-12} m² s^{-1}).

Figure 5 (A-D) shows the results of the "in-diffusion until equilibrium" experiments carried out on the compacted clay samples at four water saturation states. As for the intact sample, K_D values were at

first estimated from Eq (3) using ^{22}Na rock profile data and the last activity measurements in solution. The use of these values for modeling the activity evolution over time in solution (red line in left figures) allowed the experimental data to be well reproduced. All the corresponding diffusive parameters were reported in Table 3. Note that, independently of the water saturation degree, the equilibrium state is reached in samples, even though the higher the desaturation the longer the time to reach a plateau in solution.

Cesium in-diffusion experiments

Results obtained from "in-diffusion until equilibrium" experiments on intact rock samples at full saturation and at 81% of saturation were reported in Figure 6 (A-D). The associated simulated curves were also given and calculated using diffusive parameters given directly in Figure 6 (A &C) and also in Table 3. While the cesium concentration evolves very regularly at full saturation (Figure 6 (A)), more spreading data were acquired at 81% of saturation (Figure 6 (C)), increasing the associated uncertainties on the estimated diffusive parameters. However, a good consistency is revealed between Cs rock profile and the Cs concentration in solution.

Lastly, Figure 7 (A-H) shows the in-diffusion results for the compacted samples at four water saturation states with the associated simulations. As for the "in-diffusion until equilibrium" experiments on intact rocks, the presence of PEG in solution would lead to more spreading ^{134}Cs activity data, especially for the more concentrated one, at 70 % of saturation, which exhibits no activity decrease in solution for the first 170 days and then a rapid drop until a plateau (Figure 7 (G)). Such results from this last experiment at 70 % of saturation have to be considered cautiously, like the associated modellings.

DISCUSSION

Saturation effect on ^{22}Na adsorption behavior

All the K_D values estimated from though, out- and "in-diffusion until equilibrium" experiments on intact and compacted samples were plotted in Figure 8 as a function of the water saturation degree of the clay sample. At full saturation, all the methods led to a consistent dataset, given the associated uncertainty bars. Indeed, K_D values ranged from 0.6 mL g^{-1} for the compacted sample to 0.8 mL g^{-1} for the intact sample using though-diffusion technique.

Moreover, for intact rock samples submitted to the through-diffusion technique, the higher the desaturation, the larger the discrepancy between K_D values estimated from incoming flux in downstream reservoir and from activity decrease in upstream reservoir. Such a tendency can be originated from the fact that K_D values from incoming flux are estimated from the transient part of experiments, so that they would reflect the exchangeable ^{22}Na able to cross samples during this short period. The effect of saturation on these K_D values suggests that the stronger the desaturation, the more complex the diffusive pathway, associated to a possible creation of dead-end pores or isolated water films, capable of strongly slowing down the diffusion of ^{22}Na across samples. On the contrary, K_D values estimated from upstream reservoir would probe the total amount of ^{22}Na diffusing into samples.

In-diffusion experiment carried out until equilibrium on rock sample at 81% of saturation led a K_D value well matching the lowest part of the large K_D range estimated from upstream data evolution

during through-diffusion experiment, strengthening these previous estimations (Figure 8). Besides, comparison of K_D values estimated from out-diffusion experiments with the ones derived from through-diffusion reveals that, at 89% of saturation, out-diffusion K_D values are close to the value estimated from upstream data during through-diffusion experiment. This indicated that all the injected ^{22}Na during the through-diffusion step could be recovered by the out-diffusion step. At 86% and 81% of saturation, the K_D values derived from out-diffusion are located in Figure 8 between those derived from upstream data and in-diffusion, and those estimated from incoming flux during through-diffusion experiments. This could suggest that time spent for out-diffusion step was no enough long to recover all ^{22}Na having diffused into these samples during the through-diffusion step (^{22}Na remaining into dead-end pores, interlayer space or isolated water films) or that it would exist some irreversible processes preventing all ^{22}Na from diffusing out.

A last issue to address is how some K_D values estimated on partially-saturated samples could be higher than the ones obtained at full saturation. Could it be an effect of underestimated uncertainties or of actual processes, such as an over-concentration of the pore-water chemistry under partially saturated conditions due to dehydration? For the moment, this issue is still under debate.

Regarding K_D values estimated from in-diffusion on compacted samples, the saturation effect seems to be relatively low, K_D values ranging from 0.6 mL g^{-1} at full saturation to 0.85 mL g^{-1} at 81% of saturation. Given the associated uncertainty bars, one cannot state any influence of desaturation.

In summary, these results show that the different methods used for estimating K_D values do not probe the same mechanisms:

- The through-diffusion method using the incoming flux (down-stream reservoir) would point out the exchangeable ^{22}Na capable of crossing samples in the beginning of experiments, giving access to the most dominant or the fastest diffusive process, which would take place in the most connected pores;

- The through-diffusion method using the activity decrease in upstream reservoir only allows an estimation of all ^{22}Na diffusing into samples;

- The out-diffusion method would bring information about ^{22}Na capable of diffusing out of samples, *i.e.*, the reversible or the more mobile ^{22}Na fraction;

- The in-diffusion until equilibrium associated to post-mortem rock profile is a more accurate technique than through-diffusion using activity decrease to determine the exact amount of adsorbed ^{22}Na without any distinction between irreversible, reversible fractions, or fast or slow diffusive fractions.

Saturation effect on cesium adsorption behavior

The cesium K_D values estimated in the current study were compared in Figure 9 with cesium K_D values derived from Savoye *et al.* (2012a) as a function of the water saturation degree of the clay sample. The previous study was performed using osmotic technique on intact partially-saturated samples originated from a neighbor core. Contrary to the current diffusion approach, a transient in-diffusion method had been applied for 37 days, followed by a post-mortem analysis enabling the acquisition of cesium rock profiles. Both types of data (concentration decrease in solution and rock

profile) had been used for determining diffusive parameters, including K_D. Note that the transient in-diffusion method used by Savoye et al. (2012a) led to K_D values with larger uncertainties, since α and D_e were not adjusted independently, contrary to the 'in-diffusion until equilibrium' method.

The Savoye *et al.* (2012a)'s results did not show any clear impact of saturation on cesium adsorption (Figure 9), while the K_D values derived in the current study both on intact and compacted samples decreased when saturation degree decreased. However, such an apparent contradiction can be related to the non-linear behavior of adsorption cesium. Indeed, plotting all these K_D data as a function of their associated cesium concentrations in solution at the equilibrium reveals that the higher the cesium concentration in solution the lower the K_D values (Figure 10), as already shown by Chen *et al.* (2014) on fully-saturated intact or compacted samples originated from the Callovo-Oxfordian formation. This suggests that the non-linear cesium adsorption could be also responsible for the main features shown in Figure 9. Finally, intact and compacted samples would behave in the same manner, with an extent of saturation effect on cesium adsorption than cannot be clearly distinguished from the non-linear adsorption cesium behavior effect.

Saturation effect on cation diffusivity

Figure 11 shows the evolution of the diffusivity, *i.e.*, the ratio $D_e^{species}/D_w^{species}$ of each species as a function of the water saturation degree of the clay sample, with $D_w^{species}$ the diffusion coefficient in free water. HTO data derived from Savoye *et al.* (2010) on neighbor intact COx rock samples were also reported for comparison. Enhanced diffusion of cations was generally described as regard to the diffusivity of HTO (used as a reference) in the same sample, according to $A = (D_e/D_w)_{cations} / (D_e/D_w)_{HTO}$.

At full saturation, on intact samples, the graph clearly highlights the enhanced diffusion for the two cations with respect to tritiated water (HTO), with *A* equal to 4 and 10 for sodium and cesium, respectively. This tendency was already fully documented in literature in the same Callovo-Oxfordian formation (Melkior *et al.* 2005, 2007; Savoye *et al.* 2011, 2012a, 2015) but also in other argillaceous rocks (Van Loon & Eikenberg, 2005; Tachi et al. 2011; Gimmi & Kosakowski, 2011). Melkior *et al.* (2007) found that the respective diffusivity of alkaline cations in COx is the following Cs > Rb > K > Na > Li, as found in the current study. Enhanced diffusion for cations is also effective in compacted COx materials (ρd = 1.6 g cm^{-3}) under fully-saturated conditions with cesium diffusivity 4 times higher than the sodium one. This increased solute flux was often attributed to surface diffusion, *i.e.*, transfer of cations located in the vicinity of the charged surfaces of clay particles, in the diffuse layer or even "adsorbed" (Gimmi & Kosakowski, 2011). Relationships based on nanoscale processes were proposed to explain the macroscopic behavior of cations. Based on an experimental set of K_D and D_e data, Gimmi & Kosakowski (2011) have proposed an empirical relationship linking adsorption and diffusive behavior of cations, assuming there is only a fraction of cation located in the diffuse layer which is capable of diffusing. They introduced a parameter, called relative diffusive mobility, μs, so as to propose the relationship between *A* and K_D, as follows:

$$A = 1 + \rho_d K_D \frac{\mu_S}{\varepsilon_{HTO}} \qquad (15)$$

The application of this relationship to our data obtained on fully-saturated intact samples, led to an estimation of μ_s equal to 0.29 for sodium and 0.027 for cesium. These values are very consistent with

those estimated by Gimmi & Kosakowski (2011) from an analysis of a large data set acquired from sodium or cesium diffusion experiments on clay and clayrocks. Indeed, they estimated for sodium a μ_s median value of 0.45, with minimum and maximum values of 0.07 and 0.8, and for cesium, a μ_s median value of 0.026 with minimum and maximum values of 0.005 and 0.05. Such a high average surface mobility for ^{22}Na (*i.e.*, almost 1/3 of the mobility in bulk water) can be related to the fact that adsorbed Na cations are known to be located further away from the surfaces because of their high hydration energy. Conversely, the lower average surface mobility of cesium cations can be related to their lower hydration energy and higher affinity and thus a lower probability of a movement along the clay surface (Kim & Kirkpatrick 1997; Rotenberg *et al.* 2007; Gimmi & Kosakowski 2011, Churakov 2013).

When dehydrating clay samples under a suction of 1.9 MPa, the cesium diffusivity exhibits higher reduction (by factors of 17 and 47) with respect to fully-saturated conditions than (i) the sodium diffusivity (reduction by factors of 5.1 and 5.9) for intact and compacted samples, respectively, and (ii) the HTO diffusivity (reduction by a factor of 2.8 for intact samples) (Figure 11). However, at such suction of 1.9 MPa, the sharp diffusivity reductions for cesium and, to a lesser extent, sodium, are not accompanied by any decrease of the associated K_D values both for intact and compacted samples, as initially expected (Figure 8 and Figure 9). The application of Eq (15), using the same μ_s values as calculated at full saturation and HTO diffusive data led to overestimated theoretical values of D_e^{cation} at 1.9 MPa for intact state, *i.e.*, 2 and 6 times higher than the measured ones for sodium and cesium, respectively. In this case, K_D values required to estimate the correct D_e^{cation} values at 1.9 MPa from Eq (15) should be equal to 0.3 mL g^{-1} and 1.5 mL g^{-1}, values considerably smaller than the ones experimentally determined, *i.e.*, 0.78 mL g^{-1} and 25 mL g^{-1} for sodium and cesium, respectively.

Therefore, these results allow one to clarify the issue of the differential evolution of diffusivity for HTO and cesium as a function of saturation, raised by Savoye et al. (2012a). Indeed, the distinct diffusivity reduction observed between the three species (*i.e.*, cesium, sodium and HTO) showed that the hypothesis suggesting that HTO would be solely responsible for the differential evolution due to some evapo-concentration processes was not valid. For, in this case, cesium and sodium diffusivity should have behaved in the same way when dehydrating, contrary to what observed. Moreover, the other hypothesis assuming that the differential evolution would be due to a reduction of the clay surface accessibility to cations, and then, a reduction of the amount of adsorbed cations, when dehydrating is also largely questionable, because of the non-significant change of K_D values when dehydrating.

In fact, the distinct diffusivity evolution between sodium and cesium when dehydrating could be related to an exacerbation of differences in their diffusive behaviors still existing at full saturation. Rotenberg et al. (2007) showed by means of molecular modelling simulations of cation interactions with clay surface that, at full-saturation state, the Cs trajectories exhibited a site-to-site diffusion with very localized Cs fixation sites, while in the Na case, the motion is more diffuse, associated to outer-sphere Na complexes. This study qualitatively showed by simulations why the relative diffusive mobility, μs, of sodium was higher than that of cesium. Moreover, using molecular modelling approach, Churakov (2013) pointed out a distinct evolution with saturation of the different surface complexes for Na and Cs formed on montmorillonite surface. In the range of the suctions investigated in the current study, *i.e.*, from 0 MPa to 39 MPa (NaCl saline solution), his simulations indicated that Na ions mainly formed outer-sphere complexes, while the proportion of outer and

inner-sphere Cs complexes calculated at full-saturation (2/3 & 1/3) progressively moved to 1/3 of outer-sphere complexes and 2/3 of inner-sphere complexes. Such an evolution was associated with a reduction of the distance of Cs to the clay surface, leading to a possible decrease of its relative diffusive mobility with respect to that of Na, when dehydrating. In the end, this molecular modelling study and our experimental work clearly indicate the evolutionary behavior of the relative diffusive mobility, μ_s, of Na and Cs according to saturation, and thus, some significant changes of double layer properties when dehydrating.

SUMMARY AND CONCLUSION

The diffusion and adsorption properties of ^{22}Na and cesium have been investigated on unsaturated core of Callovo-Oxfordian (COx) claystones. Through-, out- and in-diffusion laboratory experiments have been performed on intact or compacted samples partially-saturated using the osmotic method for imposed suction up to 9 MPa. The aim was to address the issue of the unexpected differential evolution of diffusivity for the tritiated water (HTO) and cesium as a function of saturation, raised by Savoye et al. (2012a) in intact neighbor COx samples. The problem was approached by (i) adapting a method developed at full saturation to partially water saturated conditions in order to properly determine K_D value on intact or compacted samples and (ii) studying a third species, the sodium, expected to behave in an intermediate manner between cesium and HTO. The main findings and conclusion were as follows:

(1) The application of suction up to 9 MPa allowed the intact samples to be dehydrated down to 81% and the compacted samples down to 70%. Moreover, for each suction level strictly higher than 0 MPa, compacted materials display saturation degree values about 10% lower than the ones measured on the intact materials.

(2) At full saturation, a good consistency was evidenced between the K_D values estimated on intact and compacted samples for ^{22}Na and Cs, in accordance with previous studies such as the one carried out by Chen *et al.* (2014) for cesium.

(3) Independently of sample state (intact or compacted), one cannot conclude whether desaturation drastically impacted ^{22}Na adsorption, given the associated uncertainty bars. However, in details, some epiphenomena were revealed depending on the diffusion methods used for determining K_D values. The through-diffusion method using the incoming flux would point out the exchangeable ^{22}Na, capable of crossing samples in the beginning of experiments, giving access to the most dominant or the fastest diffusive process; the out-diffusion method would bring information about ^{22}Na capable of diffusing out of samples, *i.e.*, the reversible or the more mobile ^{22}Na fraction; and the "in-diffusion until equilibrium" associated to post-mortem rock profile enabled the determination of the exact amount of adsorbed ^{22}Na, without any distinction between irreversible, reversible fractions, or fast or slow diffusive fractions.

(4) For cesium, intact and compacted samples would behave in the same manner, with an extent of saturation effect on cesium adsorption than cannot be clearly distinguished from the dependence of cesium sorption to the cesium concentration in pore water.

(5) Therefore, the very small impact of saturation on the extent of adsorption for ^{22}Na and cesium would indicate that the saturation degrees were not enough low to limit the access of cations to clay surfaces (including interlayer space) onto which they could be adsorbed. Clay matrix was unlikely emptied by the highest suctions used in this study.

(6) At full saturation, enhanced diffusion for ^{22}Na and cesium was clearly evidenced on intact samples with diffusivity 4 and 10 times higher than that of tritiated water (HTO), respectively, in accordance with previous works. Even though no HTO data were acquired on compacted samples, the very large diffusivity of cesium estimated on these types of material, *i.e.*, 4 times higher than that measured for ^{22}Na clearly showed that enhanced diffusion would also take place in such compacted materials.

(7) When dehydrating clay samples, the diffusion was clearly slower than that in fully-saturated samples. Diffusivity for cesium decreased, from 0 to 1.9 MPa of suction, by factors of 17 and 47, and for sodium, by factors of 5.1 and 5.9, for intact and compacted materials, respectively. The distinct diffusivity reduction observed between each species and the non-significant change of K_D values showed the role played by desaturation for exacerbating differences in diffusive behaviors of cesium, sodium and HTO. A differential decrease of the relative diffusive mobility in diffuse layer of adsorbed cesium compared to adsorbed sodium was then proposed based on a literature review, in addition to the particular behavior of HTO, which could diffuse both in liquid and gaseous phases so as to reduce its diffusive pathways.

ACKNOWLEDGEMENT

The work focusing on the ^{22}Na through- and out-diffusion experiments on intact rocks received financial support from Andra and CEA, while the part dedicated to in-diffusion experiments received financial support from Andra.

REFERENCES

Aldaba D, Rigol A, Vidal M (2010) Diffusion experiments for estimating radiocesium and radiostrontium sorption in unsaturated soils from Spain: Comparison with batch sorption. *Journal of Hazardous Materials*, **181**, 1072–1079.

Altmann S, Aertsens M, Appelo T, Bruggeman C, Gaboreau S, Glaus M, Jacquier P, Kupcik T, Maes N, Montoya V, Rabung T, Robinet JC, Savoye S, Schaefer T, Tournassat C, Van Laer L, Van Loon LR (2015) *Processes of cation migration in clayrocks (CatClay)*, Final Scientific report. CEA-R-6410, 143 pp.

ANDRA (2005) *Dossier 2005 argile – Tome – Evolution phénoménologique du stockage géologique.* Rapport Andra no. C.RP.ADS.04.0025, France, http://www.andra.fr/download/site-principal/document/editions/182.pdf

Armand G, Leveau F, Nussbaum C, de La Vaissiere R, Noiret A, Jaeggi D, Landrein P, Righini C (2014). Geometry and properties of the excavation-induced fractures at the Meuse/Haute-Marne URL drifts. *Rock Mechanics and Rock Engineering*, **47**, 21-41.

Chen Z, Montavon G, Ribet S, Guo Z, Robinet J-C, Davida K, Tournassat C, Grambow B, Landesman C (2014) Key factors to understand in-situ behavior of Cs in Callovo-Oxfordian clay-rock (France). *Chemical. Geology*, **387**, 47–58.

Churakov SV (2013) Mobility of Na and Cs on Montmorillonite Surface under Partially Saturated Conditions. *Environmental Science and Technology*, **47**, 9816−9823.

Claret F, Sakharov BA, Drits VA, Velde B, Meunier A, Griffault E, Lanson B (2004) Clay minerals in the Meuse-Haute Marne underground Laboratory (France): possible influence of organic matter on clay mineral evolution. *Clays Clay Minerals*, **52**, 515−532.

Delage P, Howat MD, Cui YJ (1998) The relationship between suction and swelling properties in a heavily compacted unsaturated clay. *Engineered Geology*, **50**, 31-48.

Descostes M, Blin V, Bazer-Bachi F, Meier P, Grenut B, Radwan J, Schlegel M L, Buschaert S, Coelho D, Tevissen E (2008) Diffusion of anionic species in Callovo-Oxfordian argillites and Oxfordian limestones (Meuse/Haute-Marne, France). *Applied Geochemistry*, **23**, 655-677.

Fityus SG, Smith DW, Booker JR (1999) Contaminant transport through an unsaturated soil liner beneath a landfill. *Canadian Geotechnical Journal*, **36**, 330–354.

Gaucher E, Robelin C, Matray J M, Negrel G, Gros Y, Heitz J F, Vinsot A, Rebours H, Cassagnanere A, Bouchet (20047) ANDRA underground research laboratory: interpretation of the mineralogical and geochemical data acquired in the Callovian- Oxfordian formation by investigative drilling. *Physics and Chemistry of the Earth*, 29, 55−77.

Gimmi T, Kosakowski G (2011) How mobile are sorbed cations in clays and clay rocks? *Environmental Science and Technology*, **45**, 1443-1449.

Hamamoto S, Perera MSA, Resurreccion A, Kawamoto K, Hasegawa S, KomatsuT, Moldrup P (2009) The Solute Diffusion Coefficient in Variably Compacted, Unsaturated Volcanic Ash Soils. *Vadoze Zone Journal*, **8**, 942–952.

Hendry MJ, Solomon DK, Person M, Wassenaar LI, Gardner WP, Clark ID, Mayer KU, Kunimaru T, Nakata K, Hasegawa T (2015) Can argillaceous formations isolate nuclear waste? Insights from isotopic, noble gas, and geochemical profiles. *Geofluids*, **15**, 381-386.

Jakob A, Sarott F-A, Spieler P (1999) *Diffusion and sorption on hardened cement pastes – experiments and modelling results.* NAGRA NTB 99-06, Nagra, Wettingen, Switzerland, http://www.nagra.ch/documents/database/dokumente/$default/Default%20Folder/Publikationen/NTBs%201994-2000/e_ntb99-06.pdf

Kim Y, Kirkpatrick R J (1997) Na-23 and Cs-133 NMR study of cation adsorption on mineral surfaces: Local environments, dynamics, and effects of mixed cations. *Geochimica Cosmochimica Acta*, **61**, 5199–5208.

Marschall P, Horseman S, Gimmi Th (2005) Characterisation of Gas Transport Properties of the Opalinus Clay, a Potential Host Rock Formation for Radioactive Waste Disposal. *Oil Gas Science Technologie. – Revue. IFP*, **60**, 121-139

Melkior T, Yahiaoui S, Motellier S, Thoby D, Tevissen E (2005) Caesium sorption and diffusion in Bure mudrock samples. Applied Clay Science, **29**, 172-186.

Melkior T, Yahiaoui S, Thoby D, Motellier S, Barthès V (2007) Diffusion coefficients of alkaline cations in Bure mudrock. *Physics and Chemistry of the Earth*, **32**, 453–462.

Montavon G, Alhajji E, Grambow B (2006) Study of the interaction of Ni2+ and Cs+ on MX-80 bentonite; effect of compaction using the "capillary method". *Environmental Science and Technology*, **40**, 4672–4679.

Moridis GJ (1998) *A set of semi-analytical solutions for parameter estimation in diffusion cell experiments.* Report LBNL-41857, Lawrence Berkeley National Laboratory, Berkeley, California.

Rotenberg B, Marry V, Dufrêche JF, Malikova N, Giffaut E, Turq P (2007) Modelling water and ion diffusion in clays: A multiscale approach. *Comptes Rendus Chimie*, 10, 1108–1116.

Savoye S, Michelot JL, Witterbroodt C, Altinier, MV (2006) Contribution of the diffusive exchange method to the characterization of pore water in the consolidated argillaceous rocks. *Journal of . Contaminant Hydrology*, **86**, 87-104.

Savoye S, Michelot JL, Bensenouci F, Matray, JM, Cabrera J (2008) Transfers through argillaceous rocks over large space and time scales: Insights given by water stable isotopes. *Physics and Chemistry of the Earth*, **33**, S67-S74.

Savoye S, Page J, Puente C, Imbert C, Coelho D (2010) A new experimental approach for studying diffusion through an intact and unsaturated medium: A case study with Callovo-Oxfordian argillite. *Environmental Science and Technology*, **44**, 3698–3704.

Savoye S, Goutelard F, Beaucaire C, Charles Y, Fayette A, Herbette M, Larabi Y, Coelho D (2011) Effect of temperature on the containment properties of argillaceous rocks: the case study of Callovo–Oxfordian claystones. *Journal of Contaminant Hydrology*, **125**, 102–112.

Savoye S, Beaucaire C, Fayette A, Herbette M, Coelho D (2012a) Mobility of cesium through the Callovo-Oxfordian claystones under partially saturated conditions. *Environmental Science and Technology*, **46**, 2633–2641.

Savoye S, Frasca B, Grenut B, Fayette A (2012b) How mobile is iodide in the Callovo–Oxfordian claystones under experimental conditions close to the in situ ones? *Journal of Contaminant Hydrology*, **142-143**, 82-92.

Savoye S, Imbert C, Fayette A, Coelho D (2014) Experimental study on diffusion of tritiated water and anions under variable water-saturation and clay mineral content: comparison with the Callovo-Oxfordian claystones. *Geological Society, London, Special Publications*, **400**, 579-588.

Savoye S, Beaucaire C, Grenut B, Fayette A (2015) Impact of the solution ionic strength on strontium diffusion through the Callovo-Oxfordian clayrocks: An experimental and modeling study. *Applied Geochemistry*, **61**, 41–52.

Schaefer CE, Arands RR, van der Sloot HA, Kosson DS (1995) Prediction and experimental validation of liquid-phase diffusion resistance in unsaturated soils. *Journal of Contaminant Hydrology*, **20**,145–166.

Shackelford C (1991) Laboratory diffusion testing for waste disposal. *Journal of Contaminant Hydrology*, **7**, 177−217.

Tachi Y, Yotsuji K, Seida Y, Yui M (2011) Diffusion and sorption of Cs+, I− and HTO in samples of the argillaceous Wakkanai Formation from the Horonobe URL, Japan: Clay-based modeling approach. *Geochimica Cosmochimica Acta*, **75**, 6742-6759.

Tang CS, Tang AM, Cui YJ, Delage P, Schroeder C, Shi B (2001) A study of the hydro-mechanical behaviour of compacted crushed argillite. *Engineering Geology*, **3-4**, 93-103.

Tokunaga TK, Finsterle S, Kim Y, Wan J, Lanzirotti A, Newville M (2017) Ion Diffusion Within Water Films in Unsaturated Porous Media. *Environmental Science and Technology*, **51**, 4338−4346.

Van Loon LR, Soler JM, Müller W, Bradbury MH (2004) Anisotropic diffusion in layered argillaceous rock: A case study with Opalinus Clay. *Environmental Science and Technology*, **38**, 5721−5728.

Van Loon LR, Eikenberg J (2005) A high-resolution abrasive method for determining diffusion profiles of sorbing radionuclides in dense argillaceous rocks. *Applied Radiation Isotopes*, **63**, 11-21.

Vinsot A, Mettler S, Wechner S (2008) In situ characterization of the Callovo-Oxfordian pore water composition. *Physics and Chemistry of the Earth*, **33**, S75–S86.

Figure Captions

Fig. 1. Values of degree of saturation determined on rock samples having undergone the osmotic method as a function of the imposed suction.

Fig. 2. Evolution of the ^{22}Na activity in the upstream reservoir (A) and ^{22}Na normalized instantaneous fluxes (B) at different values of degree of saturation for intact materials. The solid curves were calculated using the semi-analytical solutions with the parameters specified in Table 2 from the incoming flux data (+activity evolution only for fully-saturated sample). The dotted curves were calculated from activity evolution data in upstream using the same D_e values as the ones calculated from the incoming fluxes. The dashed curves were calculated from activity evolution data in upstream using D_e values preventing the simulated incoming flux from being higher than the experimental one.

Fig. 3. Evolution of the activity in the upstream (A) and downstream (B) reservoirs of the four cells during the out-diffusion step for ^{22}Na. Decay corrections were applied with respect to the start of the through-diffusion stage. The simulated curves were calculated with the diffusive parameter values given in Table 2.

Fig. 4. Evolution of the ^{22}Na activity in the source reservoir (left) and ^{22}Na activity profile in the intact COx sample at 81% of water saturation degree (right).

Fig. 5. Evolution of the ^{22}Na activity in the source reservoir (left) and ^{22}Na activity profiles in the four compacted COx samples (right).

Fig. 6. Evolution of the cesium concentration in the source reservoir (left) and cesium concentration profiles (right) in the two intact COx samples at full-saturation and at 81% of saturation.

Fig. 7. Evolution of the cesium concentration in the source reservoir (left) and cesium concentration profile (right) in the four compacted COx samples.

Fig. 8. Comparison of K_D values for ^{22}Na determined on intact and compacted materials from through-, out-, and in-diffusion methods as a function of the water saturation degree of the clay sample.

Fig. 9. Comparison of K_D values for cesium determined on intact and compacted materials from transient in-diffusion and in-diffusion until equilibrium methods as a function of the water saturation degree of the clay sample.

Fig. 10. Evolution of the K_D values for cesium as a function of the associated cesium concentration in solution at the equilibrium.

Fig. 11. Diffusivity values for cesium, ^{22}Na, and as a function of the water saturation degree.

Table Captions

Table 1 Summary of the samples, the tracers and the type of experiments performed in this study. √ means performed.

Table 2 Values of distribution coefficient (K_D) and effective diffusion coefficient (D_e) for the though- and out-diffusion for ^{22}Na for various imposed suctions on intact materials. Values between brackets indicate the uncertainty ranges.

Table 3 Values of distribution coefficient (K_D) and effective diffusion coefficient (D_e) for the in-diffusion until equilibrium of ^{22}Na and cesium for various imposed suctions on intact and compacted materials. Values between brackets indicate the uncertainty ranges.

Sample state	Thickness (mm)	[PEG] (g/g of solution)	Applied suction (MPa)	Type of experiments			
				Through-diffusion	Out-diffusion	In-diffusion until equilibrium	Petrophysical measurement
Intact	11.13	0	0	$^{22}Na^{+}$	√		
Intact	11.16	0.42	1.9	$^{22}Na^{+}$	√		
Intact	10.96	0.76	6.3	$^{22}Na^{+}$	√		
Intact	11.15	0.95	9	$^{22}Na^{+}$	√		
Intact	6.01	0.95	9			$^{22}Na^{+}$	
Compacted	10.17	0	0			$^{22}Na^{+}$	
Compacted	9.75	0.42	1.9			$^{22}Na^{+}$	
Compacted	9.88	0.76	6.3			$^{22}Na^{+}$	
Compacted	9.93	0.95	9			$^{22}Na^{+}$	
Intact	8.60	0	0			$[Cs]_{ini}=8.7 \times 10^{-4}$ M	
Intact	2.08	0.95	9			$^{134}Cs + [Cs]_{ini}=7.6 \times 10^{-4}$ M	
Compacted	6.03	0	0			$^{134}Cs + [Cs]_{ini}=8.4 \times 10^{-4}$ M	
Compacted	3.93	0.42	1.9			$^{134}Cs + [Cs]_{ini}=7.6 \times 10^{-4}$ M	
Compacted	4.02	0.76	6.3			$^{134}Cs + [Cs]_{ini}=8.4 \times 10^{-4}$ M	
Compacted	3.88	0.95	9			$^{134}Cs + [Cs]_{ini}=7.8 \times 10^{-4}$ M	
Intact	8	0.95	9				√
Compacted	10.09	0	0				√
Compacted	10.11	0.42	1.9				√
Compacted	9.86	0.76	6.3				√
Compacted	10.09	0.95	9				√

Table 1

Sample state	Species	Diffusion method	Saturation degree (%)	K_D (mL g^{-1})	$D_e \times 10^{-11}$ (m^2 s^{-1})
Intact	$^{22}Na^+$	Through diffusion, incoming flux & upstream	0	0.79 (0.53-0.90)	4.85 (3.80-5.80)
Intact	$^{22}Na^+$	Out-diffusion upstream	0	0.70 (0.60-0.76)	5.50 (5.0-6.0)
Intact	$^{22}Na^+$	Out-diffusion downstream	0	0.75 (0.60-0.77)	5.50 (5.0-7.0)
Intact	$^{22}Na^+$	Through diffusion, incoming flux	89	0.78 (0.55-0.88)	0.95 (0.75-1.10)
Intact	$^{22}Na^+$	Through diffusion, upstream	89	0.94-1.14	0.95-1.50
Intact	$^{22}Na^+$	Out-diffusion upstream	89	0.94 (0.84-1.03)	5.00 (3.0-6.0)
Intact	$^{22}Na^+$	Out-diffusion downstream	89	1.10 (0.93-1.20)	5.50 (5.0-7.0)
Intact	$^{22}Na^+$	Through diffusion, incoming flux	86	0.48 (0.38-0.75)	0.47 (0.35-0.60)
Intact	$^{22}Na^+$	Through diffusion, upstream	86	1.05-1.60	0.47-0.80
Intact	$^{22}Na^+$	Out-diffusion upstream	86	0.71 (0.60-0.78)	0.35 (0.25-0.45)
Intact	$^{22}Na^+$	Out-diffusion downstream	86	0.97 (0.88-1.06)	0.55 (0.5-0.65)
Intact	$^{22}Na^+$	Through diffusion, incoming flux	81	0.31 (0.26-0.61)	0.28 (0.20-0.38)
Intact	$^{22}Na^+$	Through diffusion, upstream	81	1.10-1.80	0.28-0.50
Intact	$^{22}Na^+$	Out-diffusion upstream	81	0.48 (0.44-0.52)	0.15 (0.10-0.20)
Intact	$^{22}Na^+$	Out-diffusion downstream	81	0.68 (0.61-0.76)	0.30 (0.25-0.35)

Table 2

Sample state	Species	Saturation degree (%)	K_D (mL g^{-1})	$D_e \times 10^{-11}$ (m^2 s^{-1})	[Cs] at the end of experiment (mmol L^{-1} of pure water)
Intact	$^{22}Na^+$	81	1.05 (0.70-1.30)	0.25 (0.15-0.35)	
Compacted	$^{22}Na^+$	100	0.60 (0.50-0.8)	13.0 (8.0-30.0)	
Compacted	$^{22}Na^+$	81	0.85 (0.50-1.00)	2.2 (2.0-2.8)	
Compacted	$^{22}Na^+$	75.5	0.76 (0.55-0.95)	0.8 (0.7-1.2)	
Compacted	$^{22}Na^+$	70	0.63 (0.30-0.75)	0.8 (0.4-1.0)	
Intact	^{134}Cs + [Cs]	100	21 (18-25)	18 (15-20)	0.54
Intact	^{134}Cs + [Cs]	81	11 (7-16)	0.3 (0.2-2.0)	0.635
Compacted	^{134}Cs + [Cs]	100	27 (25-32)	70 (30-200)	0.50
Compacted	^{134}Cs + [Cs]	81	20 (17-32)	1.5	0.55
Compacted	^{134}Cs + [Cs]	75.5	14.5 (12-22)	0.7 (0.5-1.0)	0.685
Compacted	^{134}Cs + [Cs]	70	8.1 (5-11)	0.3 (0.3-0.5)	0.69

Table 3

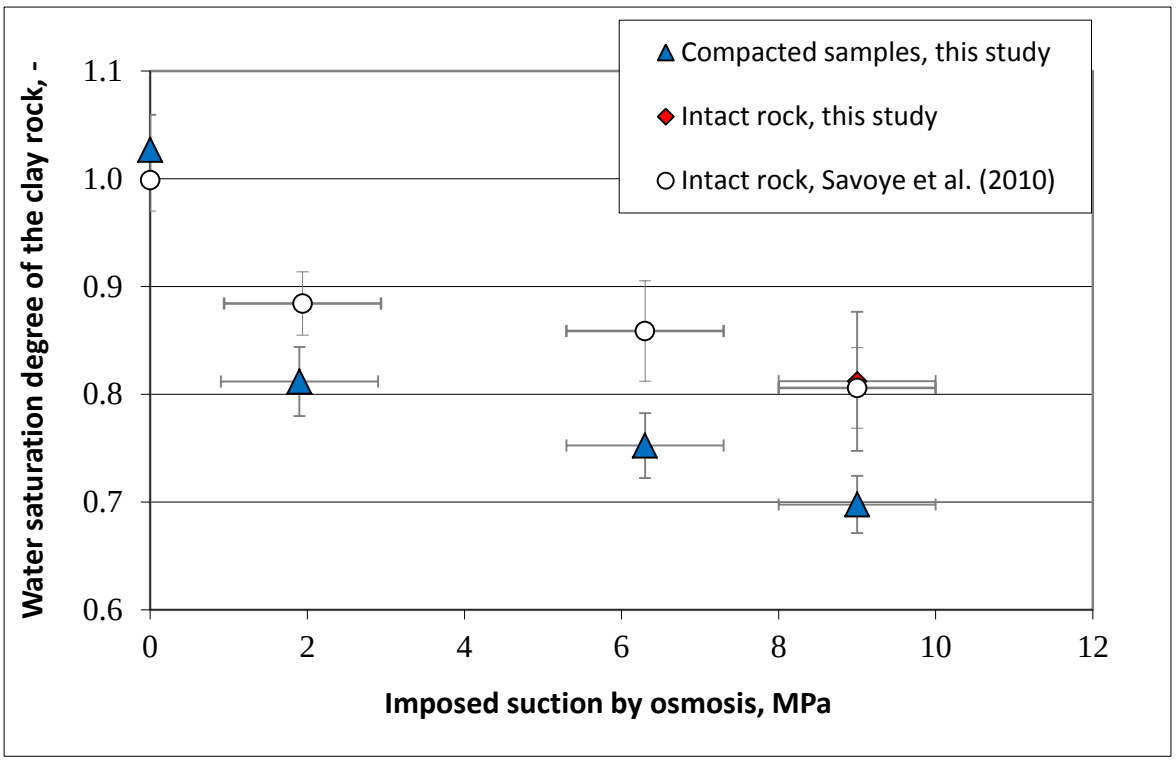
Compacted samples, this study
Intact rock, this study
Intact rock, Savoye et al. (2010)
Water saturation degree of the clay rock, -
1.1
1.0
0.9
0.8
0.7
0.6
0
2
4
6
8
10
12
Imposed suction by osmosis, MPa

Figure 1.

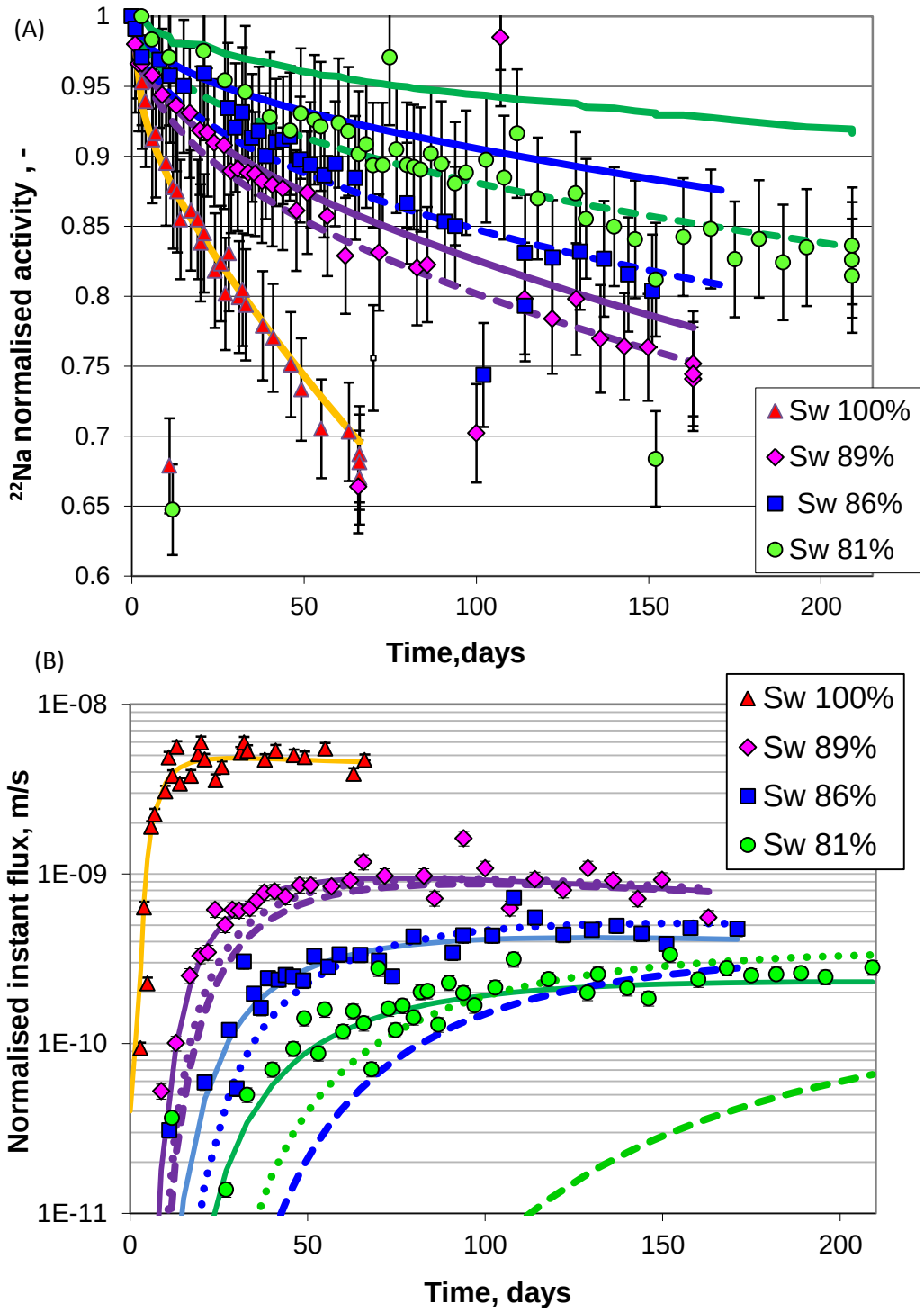
(A)
^{22}Na normalised activity , -
1
0.95
0.9
0.85
0.8
0.75
0.7
0.65
0.6
0
50
100
150
200
Time,days
Sw 100%
Sw 89%
Sw 86%
Sw 81%
(B)
Normalised instant flux, m/s
1E-08
1E-09
1E-10
1E-11
0
50
100
150
200
Time, days
Sw 100%
Sw 89%
Sw 86%
Sw 81%

Figure 2.

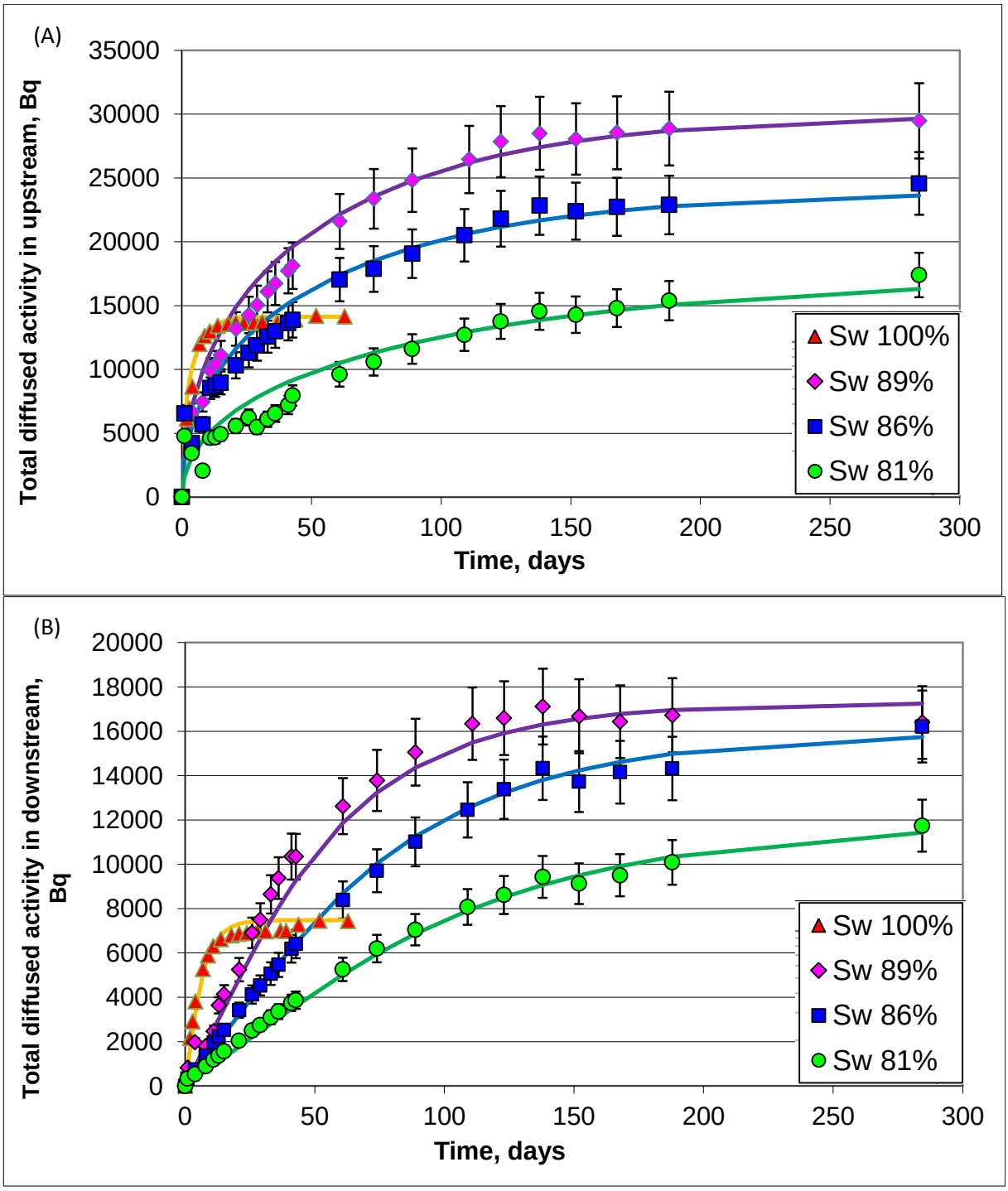
(A)
Total diffused activity in upstream, Bq
35000
30000
25000
20000
15000
10000
5000
0
0
50
100
150
200
250
300
Time, days
Sw 100%
Sw 89%
Sw 86%
Sw 81%
(B)
Total diffused activity in downstream, Bq
20000
18000
16000
14000
12000
10000
8000
6000
4000
2000
0
0
50
100
150
200
250
300
Time, days
Sw 100%
Sw 89%
Sw 86%
Sw 81%

Figure 3

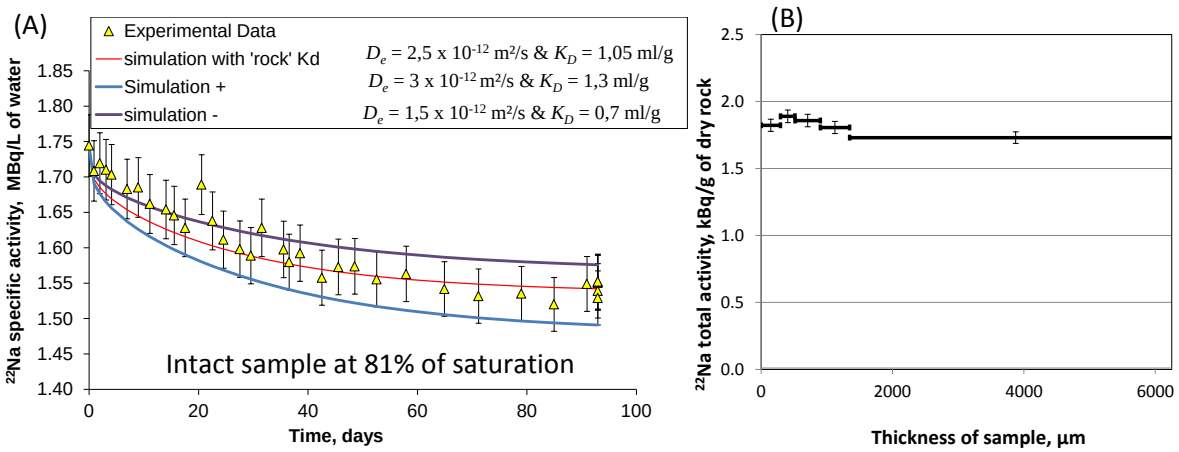
(A)
Experimental Data
simulation with 'rock' Kd
Simulation +
simulation -
D_e = 2,5 x 10^{-12} m²/s & K_D = 1,05 ml/g
D_e = 3 x 10^{-12} m²/s & K_D = 1,3 ml/g
D_e = 1,5 x 10^{-12} m²/s & K_D = 0,7 ml/g
^{22}Na specific activity, MBq/L of water
Intact sample at 81% of saturation
Time, days
(B)
^{22}Na total activity, kBq/g of dry rock
Thickness of sample, µm

Figure 4

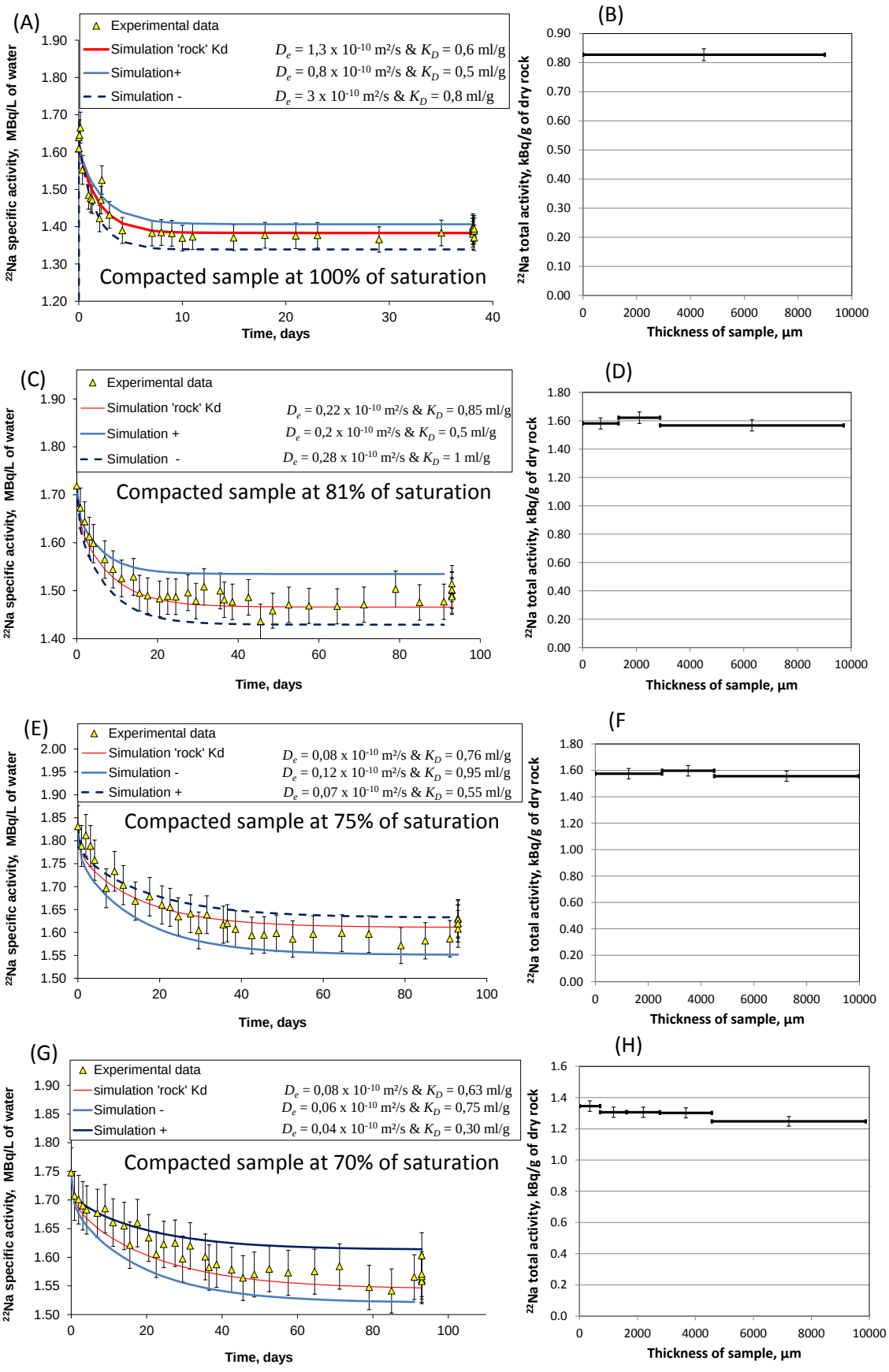
(A)
Experimental data
Simulation 'rock' Kd
Simulation+
Simulation -
D_e = 1,3 x 10^{-10} m²/s & K_D = 0,6 ml/g
D_e = 0,8 x 10^{-10} m²/s & K_D = 0,5 ml/g
D_e = 3 x 10^{-10} m²/s & K_D = 0,8 ml/g
Compacted sample at 100% of saturation
^{22}Na specific activity, MBq/L of water
Time, days
(B)
^{22}Na total activity, kBq/g of dry rock
Thickness of sample, µm
(C)
Experimental data
Simulation 'rock' Kd
Simulation +
Simulation -
D_e = 0,22 x 10^{-10} m²/s & K_D = 0,85 ml/g
D_e = 0,2 x 10^{-10} m²/s & K_D = 0,5 ml/g
D_e = 0,28 x 10^{-10} m²/s & K_D = 1 ml/g
Compacted sample at 81% of saturation
^{22}Na specific activity, MBq/L of water
Time, days
(D)
^{22}Na total activity, kBq/g of dry rock
Thickness of sample, µm
(E)
Experimental data
Simulation 'rock' Kd
Simulation -
Simulation +
D_e = 0,08 x 10^{-10} m²/s & K_D = 0,76 ml/g
D_e = 0,12 x 10^{-10} m²/s & K_D = 0,95 ml/g
D_e = 0,07 x 10^{-10} m²/s & K_D = 0,55 ml/g
Compacted sample at 75% of saturation
^{22}Na specific activity, MBq/L of water
Time, days
(F)
^{22}Na total activity, kBq/g of dry rock
Thickness of sample, µm
(G)
Experimental data
simulation 'rock' Kd
Simulation -
Simulation +
D_e = 0,08 x 10^{-10} m²/s & K_D = 0,63 ml/g
D_e = 0,06 x 10^{-10} m²/s & K_D = 0,75 ml/g
D_e = 0,04 x 10^{-10} m²/s & K_D = 0,30 ml/g
Compacted sample at 70% of saturation
^{22}Na specific activity, MBq/L of water
Time, days
(H)
^{22}Na total activity, kBq/g of dry rock
Thickness of sample, µm

Figure 5

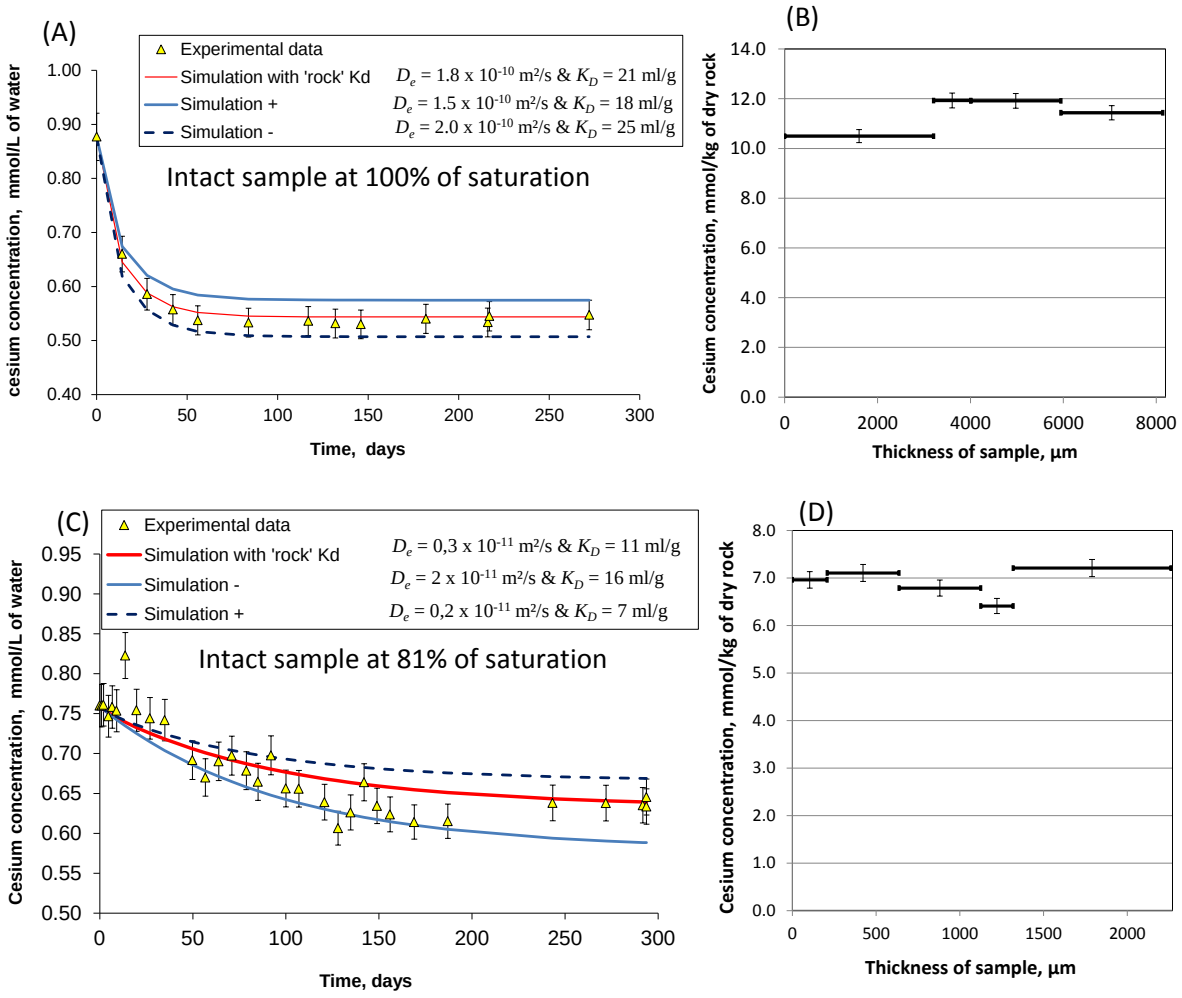
(A)
Experimental data
Simulation with 'rock' Kd
Simulation +
Simulation -
D_e = 1.8 x 10^{-10} m²/s & K_D = 21 ml/g
D_e = 1.5 x 10^{-10} m²/s & K_D = 18 ml/g
D_e = 2.0 x 10^{-10} m²/s & K_D = 25 ml/g
Intact sample at 100% of saturation
cesium concentration, mmol/L of water
Time, days
(B)
Cesium concentration, mmol/kg of dry rock
Thickness of sample, µm
(C)
Experimental data
Simulation with 'rock' Kd
Simulation -
Simulation +
D_e = 0,3 x 10^{-11} m²/s & K_D = 11 ml/g
D_e = 2 x 10^{-11} m²/s & K_D = 16 ml/g
D_e = 0,2 x 10^{-11} m²/s & K_D = 7 ml/g
Intact sample at 81% of saturation
Cesium concentration, mmol/L of water
Time, days
(D)
Cesium concentration, mmol/kg of dry rock
Thickness of sample, µm

Figure 6

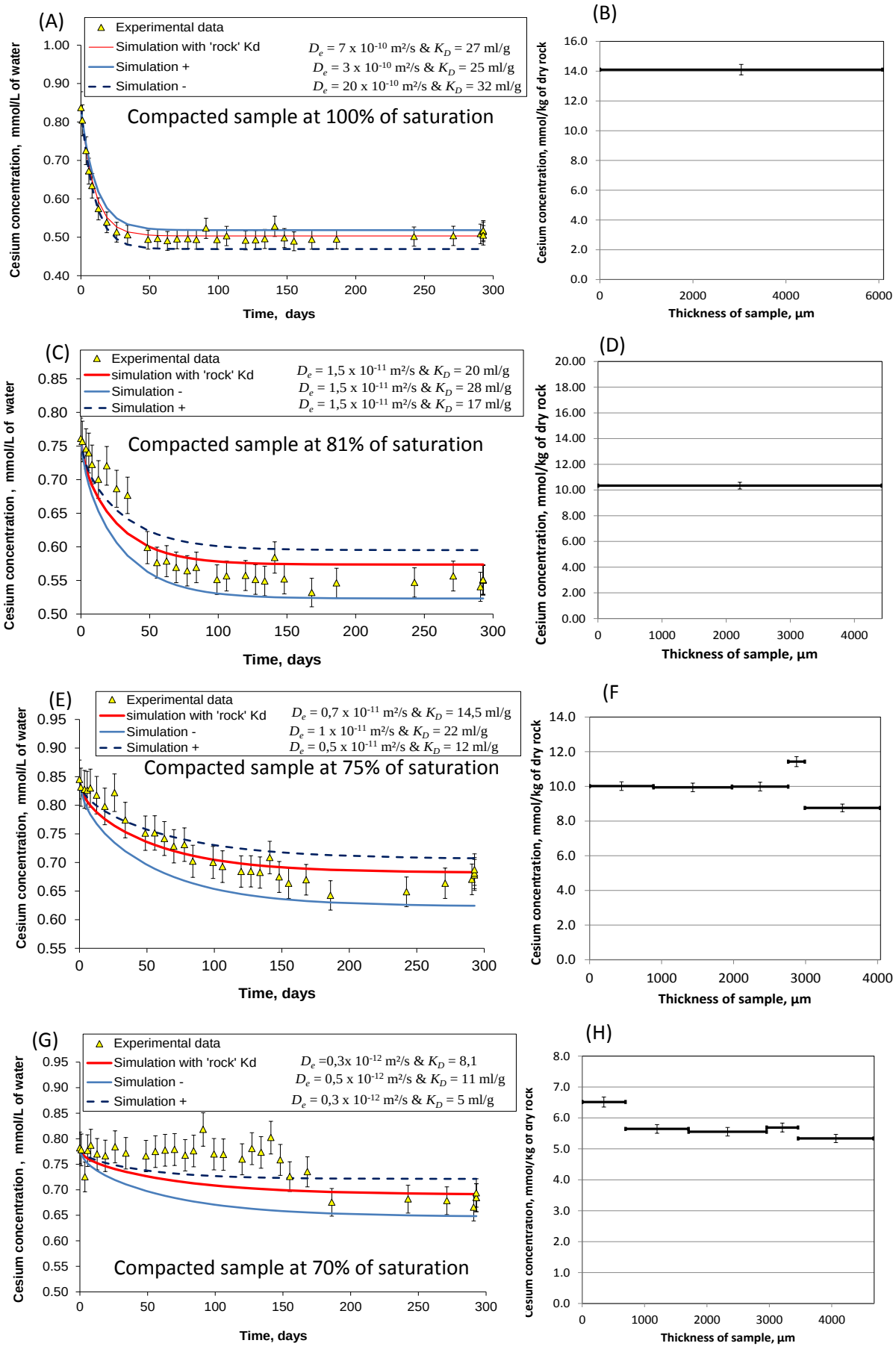
(A)
Experimental data
Simulation with 'rock' Kd
Simulation +
Simulation -
D_e = 7 x 10^{-10} m²/s & K_D = 27 ml/g
D_e = 3 x 10^{-10} m²/s & K_D = 25 ml/g
D_e = 20 x 10^{-10} m²/s & K_D = 32 ml/g
Compacted sample at 100% of saturation
Cesium concentration, mmol/L of water
Time, days
(B)
Cesium concentration, mmol/kg of dry rock
Thickness of sample, µm
(C)
Experimental data
simulation with 'rock' Kd
Simulation -
Simulation +
D_e = 1,5 x 10^{-11} m²/s & K_D = 20 ml/g
D_e = 1,5 x 10^{-11} m²/s & K_D = 28 ml/g
D_e = 1,5 x 10^{-11} m²/s & K_D = 17 ml/g
Compacted sample at 81% of saturation
Cesium concentration , mmol/L of water
Time, days
(D)
Cesium concentration, mmol/kg of dry rock
Thickness of sample, µm
(E)
Experimental data
simulation with 'rock' Kd
Simulation -
Simulation +
D_e = 0,7 x 10^{-11} m²/s & K_D = 14,5 ml/g
D_e = 1 x 10^{-11} m²/s & K_D = 22 ml/g
D_e = 0,5 x 10^{-11} m²/s & K_D = 12 ml/g
Compacted sample at 75% of saturation
Cesium concentration, mmol/L of water
Time, days
(F
Cesium concentration, mmol/kg of dry rock
Thickness of sample, µm
(G)
Experimental data
Simulation with 'rock' Kd
Simulation -
Simulation +
D_e =0,3x 10^{-12} m²/s & K_D = 8,1
D_e = 0,5 x 10^{-12} m²/s & K_D = 11 ml/g
D_e = 0,3 x 10^{-12} m²/s & K_D = 5 ml/g
Compacted sample at 70% of saturation
Cesium concentration , mmol/L of water
Time, days
(H)
Cesium concentration, mmol/kg of dry rock
Thickness of sample, µm

Figure 7

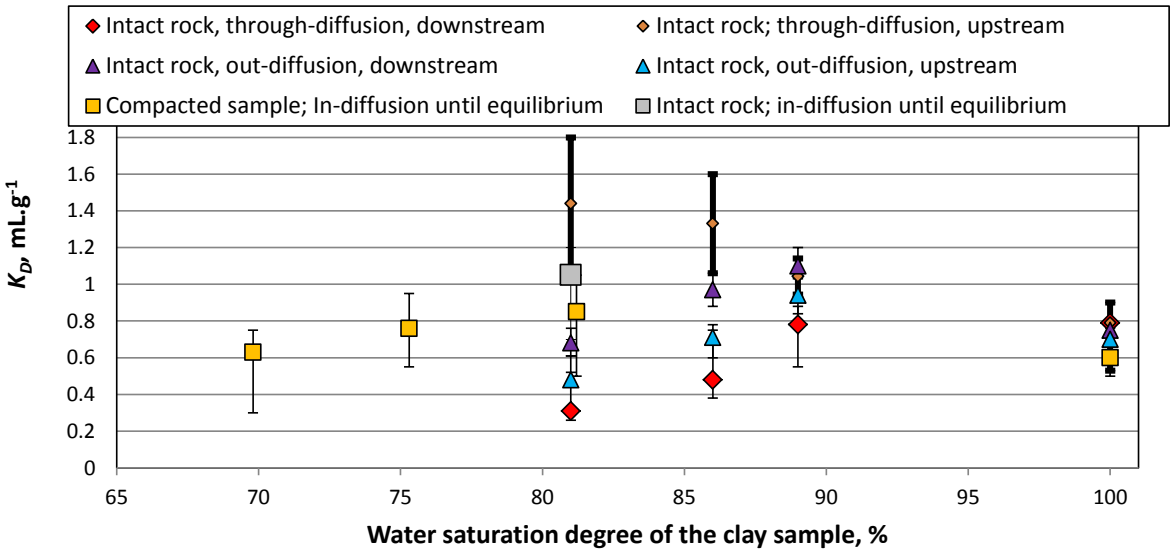
Intact rock, through-diffusion, downstream
Intact rock; through-diffusion, upstream
Intact rock, out-diffusion, downstream
Intact rock, out-diffusion, upstream
Compacted sample; In-diffusion until equilibrium
Intact rock; in-diffusion until equilibrium
K_D, mL.g^{-1}
1.8
1.6
1.4
1.2
1
0.8
0.6
0.4
0.2
0
65
70
75
80
85
90
95
100
Water saturation degree of the clay sample, %

Figure 8

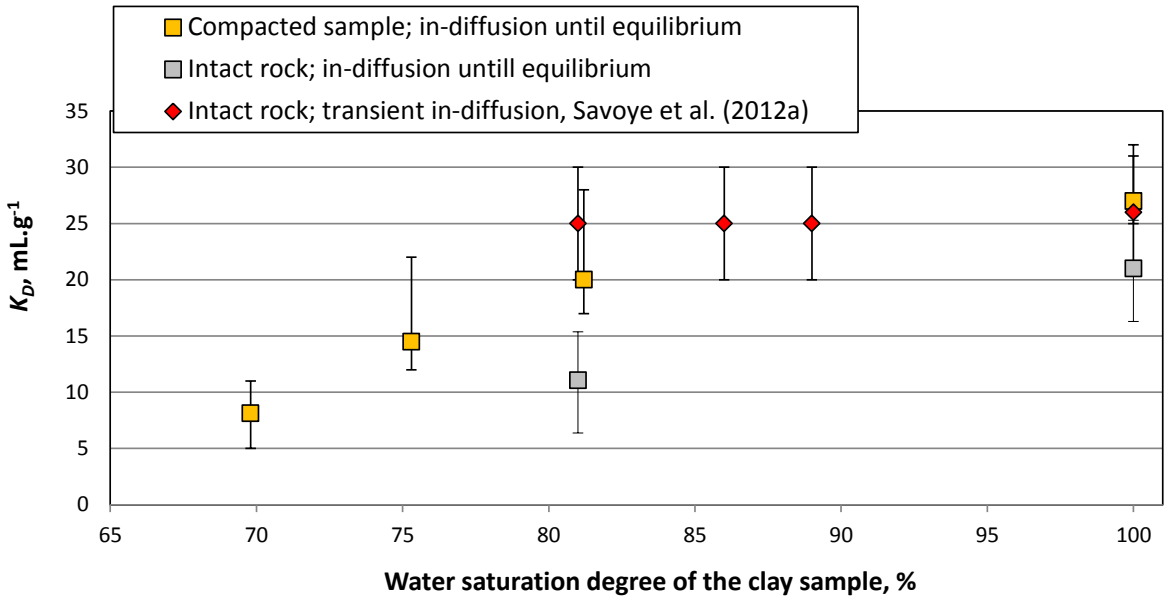
Compacted sample; in-diffusion until equilibrium
Intact rock; in-diffusion untill equilibrium
Intact rock; transient in-diffusion, Savoye et al. (2012a)
K_D, mL.g^{-1}
0
5
10
15
20
25
30
35
65
70
75
80
85
90
95
100
Water saturation degree of the clay sample, %

Figure 9

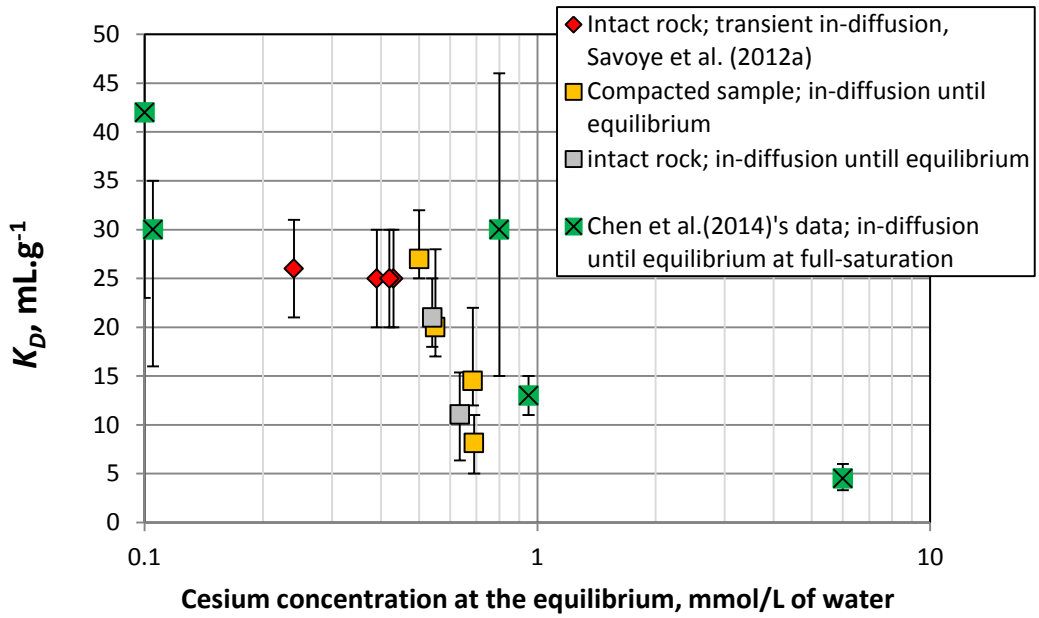
Intact rock; transient in-diffusion, Savoye et al. (2012a)
Compacted sample; in-diffusion until equilibrium
intact rock; in-diffusion untill equilibrium
Chen et al.(2014)'s data; in-diffusion until equilibrium at full-saturation
K_D, mL.g^{-1}
50
45
40
35
30
25
20
15
10
5
0
0.1
1
10
Cesium concentration at the equilibrium, mmol/L of water

Figure 10

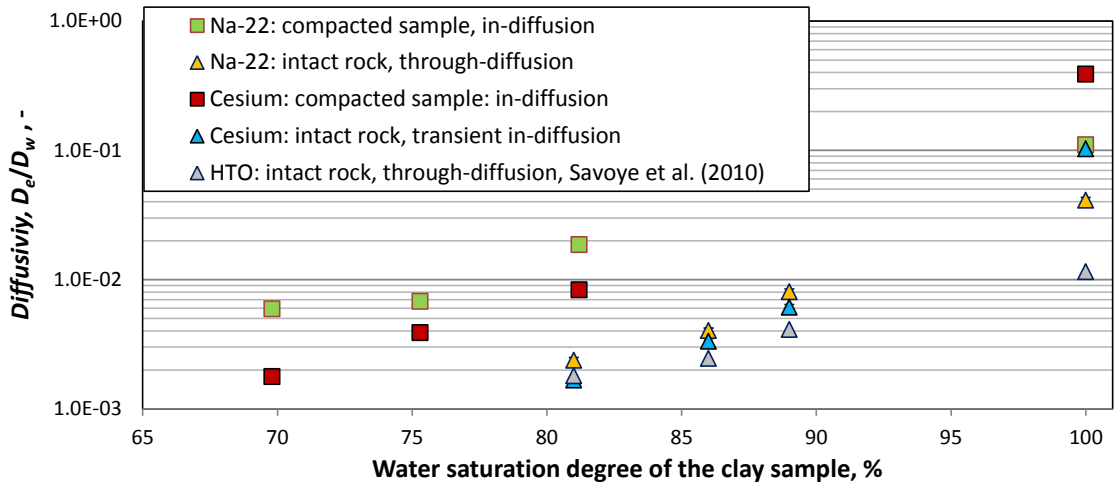
1.0E+00
1.0E-01
1.0E-02
1.0E-03
Diffusiviy, D_e/D_w, -
Na-22: compacted sample, in-diffusion
Na-22: intact rock, through-diffusion
Cesium: compacted sample: in-diffusion
Cesium: intact rock, transient in-diffusion
HTO: intact rock, through-diffusion, Savoye et al. (2010)
65
70
75
80
85
90
95
100
Water saturation degree of the clay sample, %

Figure 11.